



UNIVERSITY OF LEEDS

This is a repository copy of *Steam reforming of phenol as biomass tar model compound over Ni/Al₂O₃ catalyst*.

White Rose Research Online URL for this paper:
<http://eprints.whiterose.ac.uk/105964/>

Version: Published Version

Article:

Artexte, M, Nahil, MA, Olazar, M et al. (1 more author) (2016) Steam reforming of phenol as biomass tar model compound over Ni/Al₂O₃ catalyst. *Fuel*, 184. pp. 629-636. ISSN 0016-2361

<https://doi.org/10.1016/j.fuel.2016.07.036>

Reuse

Unless indicated otherwise, fulltext items are protected by copyright with all rights reserved. The copyright exception in section 29 of the Copyright, Designs and Patents Act 1988 allows the making of a single copy solely for the purpose of non-commercial research or private study within the limits of fair dealing. The publisher or other rights-holder may allow further reproduction and re-use of this version - refer to the White Rose Research Online record for this item. Where records identify the publisher as the copyright holder, users can verify any specific terms of use on the publisher's website.

Takedown

If you consider content in White Rose Research Online to be in breach of UK law, please notify us by emailing eprints@whiterose.ac.uk including the URL of the record and the reason for the withdrawal request.



eprints@whiterose.ac.uk
<https://eprints.whiterose.ac.uk/>

1 **Steam reforming of phenol as biomass tar model compound**
2 **over Ni/Al₂O₃ catalyst**

3 Maite Artetxe^b, Mohamad A. Nahil^a, Martin Olazar^{b*}, Paul T. Williams^a

4 ^aEnergy Research Institute, University of Leeds, Woodhouse lane, Leeds LS2 9JT,
5 United Kingdom

6 ^bDepartment of Chemical Engineering, University of the Basque Country, P.O. Box
7 644 - E48080, Bilbao, Spain

8

9 martin.olazar@ehu.es

10 Tel.: +34 946 012 527

11 Fax: +34 946 013 500

12

13 **Abstract**

14 Catalytic steam reforming of phenol over Ni/Al₂O₃ catalyst with 10 wt% of Ni loading
15 was carried out in a fixed bed reactor. The effect of temperature (650-800 °C), reaction
16 time (20-80 min) and catalyst amount (0-2 g corresponding to 0-4.5 g_{cat} h g_{phenol}⁻¹) on
17 carbon conversion, H₂ potential and catalyst deactivation was studied. High efficiency
18 of Ni/Al₂O₃ catalyst in steam reforming of phenol is observed at 750 °C for a reaction
19 time of 60 min when 1.5 g of catalyst (3.4 g_{cat} h g_{phenol}⁻¹) is used, with carbon conversion
20 and H₂ potential being 81 and 59 %, respectively. An increase in temperature enhances
21 phenol reforming reaction as well as coke gasification, minimizing its deposition over
22 the catalyst. However, at high temperatures (800 °C) an increase in Ni crystal size is
23 observed indicating catalyst irreversible deactivation by sintering. As catalyst time on
24 stream is increased the coke amount deposited over the catalyst increases, but no
25 differences in Ni crystal size are observed. An increase in catalyst amount from 0 to 1.5
26 g increases H₂ potential, but no further improvement is observed above 1.5 g. It is not
27 observed significant catalyst deactivation by coke deposition, with the coke amount
28 deposited over the catalyst being lower than 5 % in all the runs.

29

30 **Keywords:** Ni/Al₂O₃ catalyst, biomass gasification, tar model compound, phenol, steam
31 reforming

32

33

34 **1. Introduction**

35 Biomass is considered as a potential renewable energy source in order to decrease our
36 current dependence on fossil fuels [1,2]. Its abundance, renewability, carbon-neutrality
37 and low sulphur content make biomass especially interesting to replace fossil fuels as
38 energy source [3,4]. Among the different technologies, gasification is a promising one
39 in which biomass is converted into a syngas stream that can be combusted in an internal
40 combustion engine for power generation or in a furnace for heat generation [5,6].

41 Besides, the syngas produced can be used as a raw material for production of fuels and
42 chemicals by Fischer-Tropsch synthesis method [7].

43 The main drawback of biomass gasification process and its large scale implementation
44 is the formation of unwanted byproducts together with syngas, such as particulates,
45 alkali metals, fuel-bound nitrogen, sulphur, chlorine and tar [7,8]. These byproducts
46 cause several problems in process equipment (corrosion, clogging...) as well as
47 environmental pollution. Tar is a complex mixture of condensable hydrocarbons with
48 molecular weight higher than benzene and its elimination has raised significant concern
49 in literature [3,5,8-10]. The concentration and the composition of the tar in the gas
50 stream produced in biomass gasification depend on the raw material, the operating
51 conditions and the gasification technology used [11]. Tar lead to several operational
52 problems in process equipment, such as metal corrosion, clogging filters and valves or
53 condensing in cold spots plugging them. Besides, tar concentration limits the
54 application of the produced syngas in internal combustion engines ($<100 \text{ mg/Nm}^3$) as
55 well as gas turbines ($<5 \text{ mg/Nm}^3$) due to the clogging of pipelines and injectors in
56 engines and turbines [8]. Furthermore, tar compounds make the produced gas useless
57 for applications such as Fischer-Tropsch process for chemical production, in which tar
58 presence leads to serious coke deposition over the catalyst.

59 Tar removal methods can be classified in primary and secondary methods, where the
60 gas cleaning treatment is carried out inside or downstream the gasifier respectively
61 [10,12]. Several technologies have been studied for a downstream tar removal, generally
62 divided into physical methods, catalytic cracking or thermal treatment [8]. Among
63 them, downstream catalytic steam reforming is widely studied in order to convert tar
64 compounds into useful fuel gas, thus obtaining high purity gas and increasing fuel
65 value. Natural minerals, such as natural calcite, olivine and dolomite [13-16], nickel
66 based catalyst [11,17,18] or non-nickel metal catalyst [4] have been extensively studied
67 in order to find a catalyst that is inexpensive, effective in tar reduction, resistant to
68 deactivation and easily regenerated.

69 Tar model compounds are widely used in order to deeply study the catalyst performance
70 and the process operating conditions. Toluene, benzene, naphthalene and phenol are
71 usually identified as the principal biomass gasification tar model compounds [3] and
72 they are the commonly chosen tar model compounds to study its steam reforming over
73 supported metal catalysts [4,19-22]. Ni commercial steam reforming catalyst has been
74 widely studied for biomass tar reforming [8,11], given that it allows obtaining high tar
75 conversion and improving the quality of the syngas, since light hydrocarbons are also
76 reformed and higher H₂ yields are obtained. Besides, several supports (Al₂O₃, SiO₂,
77 ZrO₂, MgO, olivine...) [20,23-25] and promoters (CeO₂, Co, La...) [22,26] for Ni metal
78 have been studied in the literature in order to improve the activity, stability, coking
79 resistance and regenerability of the catalyst.

80 In this work phenol has been used as a model compound of biomass gasification tar,
81 given that it is an oxygenated aromatic compound that is more refractory to reforming
82 than non-aromatic compounds and causes faster deactivation than non-oxygenated
83 compounds. Phenol steam reforming over Ni/Al₂O₃ catalyst has been studied in order to

84 optimize the experimental conditions (temperature, reaction time, catalyst amount) for
85 maximizing the phenol conversion and minimizing the catalyst deactivation by coke
86 deposition as well as sintering. This study has been conducted with the aim of
87 optimizing operating conditions for a future detailed study of the steam reforming
88 process in which different model compounds or catalysts will be assayed. It should be
89 noted that steam reforming of phenol over Ni metal catalyst has also been studied in
90 order to obtain information about bio-oil steam reforming considering phenol as bio-oil
91 model compound [27,28].

92 **2. Experimental**

93 2.1. Catalyst preparation and characterization

94 A nickel alumina catalyst (Ni/Al₂O₃) with a nickel loading of 10 wt.% was prepared by
95 a simple impregnation method, and tested in the catalytic steam reforming of phenol.
96 Approximately 11 g of nickel nitrate hexahydrate (Ni(NO₃)₂•6H₂O, Sigma-Aldrich)
97 were dissolved in 20 ml of deionised water and mixed with approximately 20 g of
98 aluminium oxide (γ-Al₂O₃, 96% Alfa Aesar). The precursor was stirred at 100 °C for
99 around 30 minutes to ensure homogeneous mixture of components and promote water
100 evaporation. Subsequently, the resulting semi-solid mixture was further dried overnight
101 at 105 °C, and calcined at 750 °C with 20 °C min⁻¹ heating rate in an air atmosphere for
102 3 hours. The resulting catalyst was crushed and sieved to obtain finer particles with a
103 size in the 0.18-0.24 mm range. The prepared catalyst was not reduced, since during the
104 process some of the pyrolysis gases, such as H₂ and CO, have the capability to reduce
105 the catalyst itself [29].

106 The physical or structural properties of the catalyst (BET surface area, pore volume and
107 pore size distribution) were measured using Micromeritics TriStar 3000. These

108 properties were determined by the adsorption-desorption of N₂ at -192 °C. The
109 experimental procedure consists in degassing the sample for approximately 8 h at 150
110 °C to remove all possible impurities, followed by adsorption-desorption of N₂. The
111 surface area was calculated using the BET method and the average pore diameter was
112 calculated using the BJH method, with the calculated values being 116.5 m²/g and 24 Å,
113 respectively.

114 X-Ray diffraction (XRD) analyses of the catalyst were carried out using Bruker D8
115 instrument with a CuK α radiation for a qualitative phase analysis (fresh catalyst) and
116 crystal size determination (used catalyst). The samples were ground to less than 75 μ m
117 size and loaded into the 20 mm aperture of an aluminium sample holder. Concerning the
118 fresh catalyst, 3 different phases corresponding to NiO, Al₂O₃ and NiAl₂O₄ have been
119 identified. The determinations of Ni crystal size for used catalysts were carried out
120 using Scherrer equation.

121 Temperature programmed oxidation (TPO) of used catalysts were carried out to
122 determine the amount and nature of the coke deposited over the catalyst for which the
123 thermogravimetric analyzer Shimadzu TGA-50 was used. About 20 mg of sample was
124 heated in air atmosphere at 15 °C min⁻¹ to a final temperature of 800 °C and maintained
125 for 10 min at this temperature. Besides, high resolution scanning electron microscopy
126 (SEM, Hitachi SU8230) was used to identify the nature of the coke deposited over the
127 catalyst.

128 2.2. Experimental equipment and procedure

129 Figure 1 shows the experimental equipment used to study the steam reforming of phenol
130 over Ni/Al₂O₃ catalyst with 10 wt% of Ni loading. Phenol was dissolved in water at a
131 steam/carbon molar ratio of 13, and they were fed continuously by means of a syringe
132 pump using a flow rate of 6.64 ml min⁻¹. The first furnace was maintained at 250 °C to

133 evaporate the feedstock before entering the second reactor. Besides, 80 ml min^{-1} of
134 nitrogen was fed to sweep the volatiles formed in the reactor. Both reactors were 16 cm
135 length with an internal diameter of 2.2 cm and each was separately heated externally by
136 an electrical furnace. The influence of the reforming reactor temperature was studied in
137 the 650-800 °C range, using 1 g of Ni/Al₂O₃ catalyst for a reaction time of 40 min. As
138 aforementioned, the catalyst has not been reduced before use because H₂ and CO are
139 present in the reaction medium and, as concluded in a previous work [30], they are
140 capable of reducing the catalyst. Therefore, the effect of the reaction time (20-80 min)
141 was studied to analyze the evolution of catalyst activity by using 1 g of Ni/Al₂O₃ at a
142 reforming temperature of 750 °C. Moreover, the influence of the catalyst amount on
143 phenol conversion was analyzed in the 0-2 g range (corresponding to space-times in the
144 0-4.5 $\text{g}_{\text{cat}} \text{h g}_{\text{phenol}}^{-1}$ range) at 750 °C for 60 min.

145 **Figure 1**

146 The volatile stream formed goes to a condensation system which is formed by two
147 condensers cooled with dry-ice. The non-condensable gases are collected in a 10 L
148 TeldarTM gas sample bag. The gases are collected for 20 min subsequent to the end of
149 each run to ensure that all the produced gases are collected. The gases collected in the
150 gas sample bag were analysed off-line by gas chromatography. Hydrocarbon gases
151 (from C₁ to C₄) were determined by a Varian 3380 chromatograph with a flame
152 ionisation detector (GC/FID), 80-100 mesh Hysep column and using nitrogen as carrier
153 gas. Permanent gases, i.e., CO, O₂, N₂ and H₂, were determined by a Varian 3380
154 chromatograph with a 60-80 mesh molecular sieve column and argon as carrier gas with
155 a thermal conductivity detector, whereas CO₂ was analysed by another Varian 3380 GC
156 provided with a Hysep 80-100 mesh column and using argon as carrier gas and a
157 thermal conductivity detector.

158 The condensers were weighed before and after each run to measure the liquid amount
159 obtained and N₂ was used as internal standard to calculate the gas yield. Each run was
160 repeated at least twice to verify the reproducibility of the results and the mass balance
161 closure was between 95-105 % in all the runs.

162 The overall reaction of catalytic steam reforming of phenol is defined as follows:



164 In order to analyze the effect of operating conditions on the steam reforming of phenol,
165 carbon conversion and H₂ potential was defined. The carbon conversion was defined as
166 the moles of carbon in the gaseous products divided by the moles of carbon fed and H₂
167 potential as percentage of the potential stoichiometric H₂ yield, where stoichiometric H₂
168 moles were calculated according to eq. 1.

$$169 \text{C conversion (\%)} = \frac{\text{moles of carbon in the product gas}}{\text{moles of carbon in the feed}} 100 \quad (2)$$

$$170 \text{H}_2 \text{ potential} = \frac{\text{moles of H}_2 \text{ in the product gas}}{\text{moles of H}_2 \text{ in stoichiometric potential}} 100 \quad (3)$$

171 The yield of gas compounds was calculated as follows,

$$172 \text{Yield (\%)} = \frac{\text{g of the compound in the product gas}}{\text{g of phenol fed}} 100 \quad (4)$$

173 **3. Results**

174 3.1. Effect of temperature

175 Figure 2 shows the effect of temperature on carbon conversion and H₂ potential
176 obtained in the steam reforming of phenol over Ni/Al₂O₃ catalyst (1 g of catalyst
177 corresponding to a space time of 2.25 g_{cat} h g_{phenol}⁻¹). It can be seen that temperature has

178 great influence on phenol reforming, increasing the carbon conversion from 8 % at 650
179 °C to 57 % at 800 °C. Likewise, H₂ potential increases as reforming temperature is
180 increased, reaching a value of 47 % at 800 °C. This increase in carbon conversion and
181 H₂ potential can be attributed to the endothermic nature of oxygenated compound
182 reforming reaction, which is enhanced as temperature is increased.

183

Figure 2

184 The same trend of carbon conversion and H₂ yield with temperature was observed in the
185 literature on steam reforming of phenol over Ni/Al₂O₃ catalyst [28,31]. Wang et al. [28]
186 studied the steam reforming of different bio-oil model compounds, in which phenol has
187 been identified as the most refractory compound due to its stable structure with an
188 aromatic ring.

189 Figure 3 displays the effect of temperature on the yield of the gas compounds. It can be
190 seen that an increase in temperature increases the yield of all gas compounds due to the
191 enhancement of reforming reaction, reaching a maximum CO₂, CO and H₂ yield at 800
192 °C, 66, 55 and 14 wt%, respectively. Phenol steam reforming reaction on nickel surface
193 is explained by two possible mechanisms [32], which are initiated with the dissociation
194 of O-H followed by: i) a ring opening caused by C-H scission and C=C rupture in
195 positions 2 and 6; ii) C-O bond dissociation followed by C-H and C=C rupture. Both
196 decomposition mechanisms give way to H₂, CO and light hydrocarbon formation. The
197 low values of light hydrocarbon yields obtained (lower than 1 wt% in all the
198 temperature range studied) shows that its reforming is almost complete even at low
199 temperatures. The low CH₄ yield obtained can be attributed to the absence of methyl
200 group in the phenol structure.

201

Figure 3

202 Nevertheless, it can be observed that the ratio between CO and CO₂ is significantly
203 changed as temperature is increased, showing that an increase in temperature increases
204 the phenol reforming reaction and causes thermodynamic equilibrium displacement in
205 the water gas shift exothermic reaction.

206 Figure 4 shows the temperature programmed oxidation (DTG-TPO) curves for the coke
207 deposited over Ni/Al₂O₃ catalyst used in the steam reforming of phenol at different
208 temperatures. Ni/Al₂O₃ catalyst deactivation by coke deposition has been widely
209 studied in the literature [33,34] for which two types of coke have been identified: i)
210 amorphous coke, which is burnt at low temperatures (around 450 °C) since its
211 combustion is activated by Ni metal on which the coke is deposited causing its
212 encapsulation; ii) filamentous coke, which is not adsorbed over Ni sites and it is
213 combusted at high temperatures (above 450 °C).

214 **Figure 4**

215 The coke deposited over the catalyst used at 650 °C (4.6 wt%) is combusted in a wide
216 temperature range, between 350 and 600 °C. Although a main peak at 480 °C is
217 observed, several shoulders can be observed at different temperatures (370, 410 and 460
218 °C), which evidence the heterogeneous nature of the coke deposited. This heterogeneity
219 reveals the existence of nascent coke (the shoulder at 370 °C), which is formed by
220 phenol condensation and adsorbed as phenate species over Ni sites [35] and its
221 combustion is catalyzed by Ni metal sites. This coke evolves into more condensate
222 structures by multilayer growing and it is separated progressively from Ni sites,
223 requiring higher temperatures for its combustion.

224 Furthermore, the composition of the coke deposited in steam reforming depends on the
225 operating conditions used (temperature, steam/carbon ratio and space-time) since coke
226 deposition is a result of a balance between its formation and its elimination by

227 gasification [36]. Consequently, the coke deposited at 750 °C is significantly affected by
228 gasification, which is faster for the less condensed coke. Thus, at 750 °C the coke
229 amount deposited is lower (2.1 wt%) and more evolved, with the peak being moved at
230 higher temperatures. Coke gasification rate is higher at 800 °C, decreasing the amount
231 of coke deposited until 1.1 wt%.

232 Figure 5 shows SEM images for the fresh (a) and used catalyst (at 650 (b), 750 (c) and
233 800 (d)). It can be seen that SEM images do not show the presence of high structured
234 filamentous coke. It should be noted that the catalyst with the highest coke amount is
235 that used at the lowest temperature, for which an amorphous coke deposited between
236 catalyst particles is observed.

237 **Figure 5**

238 XRD analysis for the catalyst used in the reforming of phenol at 650 °C, 750 °C and 800
239 °C have been carried out in order to study the influence of the reforming temperature on
240 the Ni crystal size. The catalyst used at 650 °C does not present a peak representative of
241 Ni metal, indicating that 650 °C is not high enough to reduce the catalyst. The catalyst
242 used at 750 °C presents a peak representative of the Ni metal with a crystal size of 45 Å.
243 Likewise, for the catalyst used at 800 °C a peak characteristic of Ni metal is observed
244 with a crystal size of 72 Å, showing that reforming temperature causes catalyst
245 irreversible deactivation by Ni metal sinterization.

246 3.2. Effect of time on stream

247 Figure 6 displays the effect of reaction time on carbon conversion and H₂ potential
248 obtained in the catalytic reforming of phenol over Ni/Al₂O₃ catalyst at 750 °C (1 g of
249 catalyst corresponding to a space time of 2.25 g_{cat} h g_{phenol}⁻¹). It can be seen that an
250 increase in time on stream until 60 min gives way to a linear increase in carbon

251 conversion, increasing from 35 % for 20 min to 56 % for 60 min. Above 60 min no
252 change in carbon conversion is observed. As aforementioned, the catalyst is not reduced
253 before use because H₂ and CO present in the reaction medium will reduce it [37]. It can
254 be seen that an initial period of catalyst activation is necessary and the catalyst is
255 reduced completely for the run carried out for 60 min, maintaining its activity above this
256 reaction time. Similarly, H₂ potential increases as time on stream increased, reaching a
257 maximum value of 39 % for the run carried out for 40 min and maintaining this value
258 for longer reaction times.

259 **Figure 6**

260 Figure 7 shows the effect of reaction time in the catalytic reforming of phenol over
261 Ni/Al₂O₃ catalyst at 750 °C on the individual gas compounds yields obtained. It can be
262 seen that an increase in reaction time until 40 min gives way to an increase in CO, CO₂
263 and H₂ yield (47, 58, 11 %) due to the enhancement of reforming reaction as the catalyst
264 is reduced. An increase in reaction time from 40 to 60 min shows a significant increase
265 in CO₂ yield (form 58 % to 73 %) and a slight increase in H₂ yield (form 11 % to 12 %).
266 However, an increase in reaction time from 60 to 80 min gives way to a decrease in CO₂
267 (form 73 % to 63 %) and H₂ yield (form 12 % to 11 %), but an increase in the yield of
268 CO (form 49 % to 57 %). The trend observed can be attributed to water gas shift
269 reaction, which is enhanced when time on stream increases form 40 to 60 min due to the
270 complete reduction of the catalyst and an increase in its activity. However, it seems that
271 an increase in reaction time above 60 min reduces the catalyst activity for water gas
272 shift reaction since coke deposition over the catalyst decrease its activity for this
273 reaction.

274 **Figure 7**

275 DTG-TPO results for the Ni/Al₂O₃ catalyst used in phenol steam reforming at 750 °C
276 for different reaction times (Figure 8) show that the coke amount increases as reaction
277 time is increased, from 2.1 % for 20 min to 3.8 % for 80 min. It can be seen that the
278 coke deposited over all the catalysts studied is combusted between 350-600 °C and they
279 present a prevailing peak around 500 °C. Nevertheless, the nature of the coke deposited
280 over the catalyst is different depending on the reaction time. The catalyst used for 60
281 min presents a significant shoulder at low temperatures (400 °C) and a main peak at
282 intermediate temperatures (500 °C). Although the coke amount does not increase
283 significantly, an increase in reaction time until 80 min gives way to a higher degree of
284 structuring of the carbonaceous material deposited, which decreases the shoulder at low
285 temperatures (400 °C) and increases the main peak at higher temperatures (500 °C).

286 **Figure 8**

287 SEM analysis for the fresh (Figure 9a) and the catalyst used for different reaction times,
288 40 (Figure 9b), 60 (Figure 9c) and 80 min (Figure 9d), have been carried out in order to
289 gain knowledge about the coke nature and position. Regarding the SEM images, no
290 significant differences are observed for low times on stream due to the low coke amount
291 deposited over the catalyst. However, for long reaction times (Figure 11d), an
292 amorphous coke deposited is clearly observed over catalyst particles. XRD analysis has
293 also been used to calculate the Ni crystal size and analyze the influence of the reaction
294 time over catalyst deactivation by sintering. The catalysts used for 40, 60 and 80 min
295 have been analyzed and no influence of reaction time over catalyst sinterization is
296 observed, with the Ni crystal size being around 45 Å for all the catalysts studied. This
297 evidences that there is no Ni particle dragging, which is consistent with the absence of
298 filamentous coke.

299 **Figure 9**

300 3.3. Effect of catalyst amount

301 Figure 10 displays the effect of the catalyst amount used (0, 1, 1.5 and 2 g of catalyst
302 corresponding to space times of 0, 2.25, 3.4 and 4.5 $\text{g}_{\text{cat}} \text{h g}_{\text{phenol}}^{-1}$) on carbon conversion
303 and H_2 yield obtained at 750 °C and for a reaction time of 60 min (a steam/carbon molar
304 ratio of 13 and a flowrate of 6.64 ml min^{-1}). The run without catalyst was carried out
305 using 1 g of sand. As observed, the catalyst used is highly efficient, given that it
306 increases carbon conversion from 9 to 56 % and H_2 yield from 4 to 38 % when 1 g of
307 catalyst is added. An increase in the catalyst amount used from 1 to 1.5 g leads to a
308 significant increase in carbon conversion as well as H_2 potential, reaching values of 81
309 and 59 %, respectively. However, an increase in catalyst amount above 1.5 g does not
310 show a notable influence in phenol reforming, maintaining carbon conversion and H_2
311 yield almost constant when catalyst amount is increased to 2 g. Wang et al. [28]
312 obtained similar results studying the steam reforming of bio-oil model compounds over
313 Ni/ Al_2O_3 catalyst.

314 **Figure 10**

315 Figure 11 shows that an increase in catalyst amount from 0 to 1.5 g gives way to a
316 increase in the yield of CO, CO_2 and H_2 from 10, 9.9 and 1.4 wt.% to 72, 111 and 17
317 wt.%, respectively. However, an increase in space-time above this value lead to an
318 increase in the yield of CO_2 (118 wt.%) and a decrease in the yield of CO (68 wt.%),
319 indicating that water gas shift reaction is favoured when a large amount of catalyst is
320 used. Swierczynski et al. [38] have also seen the enhancement of water gas shift
321 reaction when space-time is increased. They study toluene steam reforming over
322 Ni/olivine catalyst at 800 and 650 °C showing that an increase in space-time led to an
323 increase in CO_2 selectivity and a decrease in CO selectivity.

324 **Figure 11**

325 Figure 12 displays TPO curves of the coke deposited over Ni/Al₂O₃ catalyst in the
326 steam reforming of phenol when different amounts of catalyst are used at 750 °C for 60
327 min. It can be observed that the amount of catalyst used does not affect significantly the
328 nature of the coke deposited but it does the amount of coke deposited over the catalyst.
329 All the TPO curves present a main peak at 500 °C with a shoulder at 400 °C which
330 evidences that the coke deposited over the catalyst has a similar degree of graphitization
331 and similar location over the catalyst. Furthermore, as the amount of catalyst (catalytic
332 bed length) is increased, the amount of coke deposited on the catalyst decreases.
333 Consequently, based on the evolution of phenol concentration with catalyst amount, the
334 role of phenol should be noted as coke precursor by phenate species adsorbed as
335 intermediates [35].

336 **Figure 12**

337 **4. Conclusion**

338 High carbon conversion and H₂ potential has been obtained in the steam reforming of
339 phenol over Ni/Al₂O₃ catalyst, reaching a value of 81 and 59 %, respectively, at 750 °C
340 for a reaction time of 60 min and using 1.5 g of catalyst. The coke deposited over the
341 catalyst is mainly of low degree of graphitization and its amount has been lower than 5
342 % in the whole operating range studied.

343 An increase in temperature gives way to an increase in carbon conversion and H₂
344 potential due to the enhancement of phenol reforming reaction. Besides, coke
345 gasification rate increases as temperature is increased, and the amount of coke deposited
346 over the catalyst significantly decreases (from 4.6 % to 1.1 %) when temperature is
347 increased from 650 to 800 °C. However, a high reforming temperature (800 °C) causes
348 an increase in Ni crystal size and, therefore, catalyst deactivation by sintering.

349 It is concluded that an initial period of NiO reduction is required to activate the catalyst.
350 Thus, an increase in time on stream increases the carbon conversion and H₂ potential
351 until 60 min of time on stream, from which the catalyst activity is maintained constant.
352 Regarding coke deposition, an increase in time on stream influences the amount of coke
353 deposited but also the nature of the coke, whose amount and graphitization degree is
354 higher as reaction time increases.

355 The amount of the catalyst used has great influence on phenol steam reforming, with
356 carbon conversion increasing linearly, as well as H₂ potential, with the amount of
357 catalyst used. However, phenol conversion seems to have a ceiling value in the steam
358 reforming, whereas a further enhancement of water gas shift reaction is observed.

359

360 **Acknowledgments**

361 Maite Artetxe thanks the University of the Basque Country UPV/EHU for her post-
362 graduate Grant (UPV/EHU 2013). We also acknowledge support from the UK
363 Engineering & Physical Sciences Research Council through Supergen Bioenergy Grant
364 EP/M013162/1.

365

366

367 **Reference List**

- 368 [1] Demirbas A. Biofuels sources, biofuel policy, biofuel economy and global biofuel
369 projections. *Energy Convers Manage* 2008;49:2106-16.
- 370 [2] Vassilev SV, Vassileva CG, Vassilev VS. Advantages and disadvantages of composition
371 and properties of biomass in comparison with coal: An overview. *Fuel* 2015;158:330-
372 50.
- 373 [3] Shen Y, Yoshikawa K. Recent progresses in catalytic tar elimination during biomass
374 gasification or pyrolysis-A review. *Renewable Sustainable Energy Rev* 2013;21:371-92.
- 375 [4] Li D, Tamura M, Nakagawa Y, Tomishige K. Metal catalysts for steam reforming of tar
376 derived from the gasification of lignocellulosic biomass. *Bioresour Technol*
377 2015;178:53-64.
- 378 [5] Asadullah M. Barriers of commercial power generation using biomass gasification gas: A
379 review. *Renewable Sustainable Energy Rev* 2014;29:201-15.
- 380 [6] Heidenreich S, Foscolo PU. New concepts in biomass gasification. *Prog Energy Combust*
381 *Sci* 2015;46:72-95.
- 382 [7] Choudhury HA, Chakma S, Moholkar VS. Chapter 14 - Biomass Gasification Integrated
383 Fischer-Tropsch Synthesis: Perspectives, Opportunities and Challenges. In: Sukumaran
384 APBS, editor. *Recent Advances in Thermo-Chemical Conversion of Biomass*. Boston:
385 Elsevier; 2015. p. 383-435.
- 386 [8] Anis S, Zainal ZA. Tar reduction in biomass producer gas via mechanical, catalytic and
387 thermal methods: A review. *Renewable Sustainable Energy Rev* 2011;15:2355-77.
- 388 [9] Asadullah M. Biomass gasification gas cleaning for downstream applications: A
389 comparative critical review. *Renewable Sustainable Energy Rev* 2014;40:118-32.
- 390 [10] Devi L, Ptasiński KJ, Janssen FJJG. A review of the primary measures for tar elimination
391 in biomass gasification processes. *Biomass Bioenergy* 2003;24:125-40.
- 392 [11] Chan FL, Tanksale A. Review of recent developments in Ni-based catalysts for biomass
393 gasification. *Renewable Sustainable Energy Rev* 2014;38:428-38.
- 394 [12] Goransson K, Soderlind U, He J, Zhang W. Review of syngas production via biomass
395 DFBGs. *Renewable Sustainable Energy Rev* 2011;15:482-92.
- 396 [13] Constantinou DA, Efstathiou AM. The steam reforming of phenol over natural calcite
397 materials. *Catal Today* 2009;143:17-24.
- 398 [14] Devi L, Ptasiński KJ, Janssen FJJG, van Paasen SVB, Bergman PCA, Kiel JHA. Catalytic
399 decomposition of biomass tars: use of dolomite and untreated olivine. *Renewable*
400 *Energy* 2005;30:565-87.
- 401 [15] Erkiaga A, Lopez G, Amutio M, Bilbao J, Olazar M. Steam gasification of biomass in a
402 conical spouted bed reactor with olivine and γ -alumina as primary catalysts. *Fuel*
403 *Process Technol* 2013;116:292-9.
- 404 [16] Tuomi S, Kaisalo N, Simell P, Kurkela E. Effect of pressure on tar decomposition activity
405 of different bed materials in biomass gasification conditions. *Fuel* 2015;158:293-305.

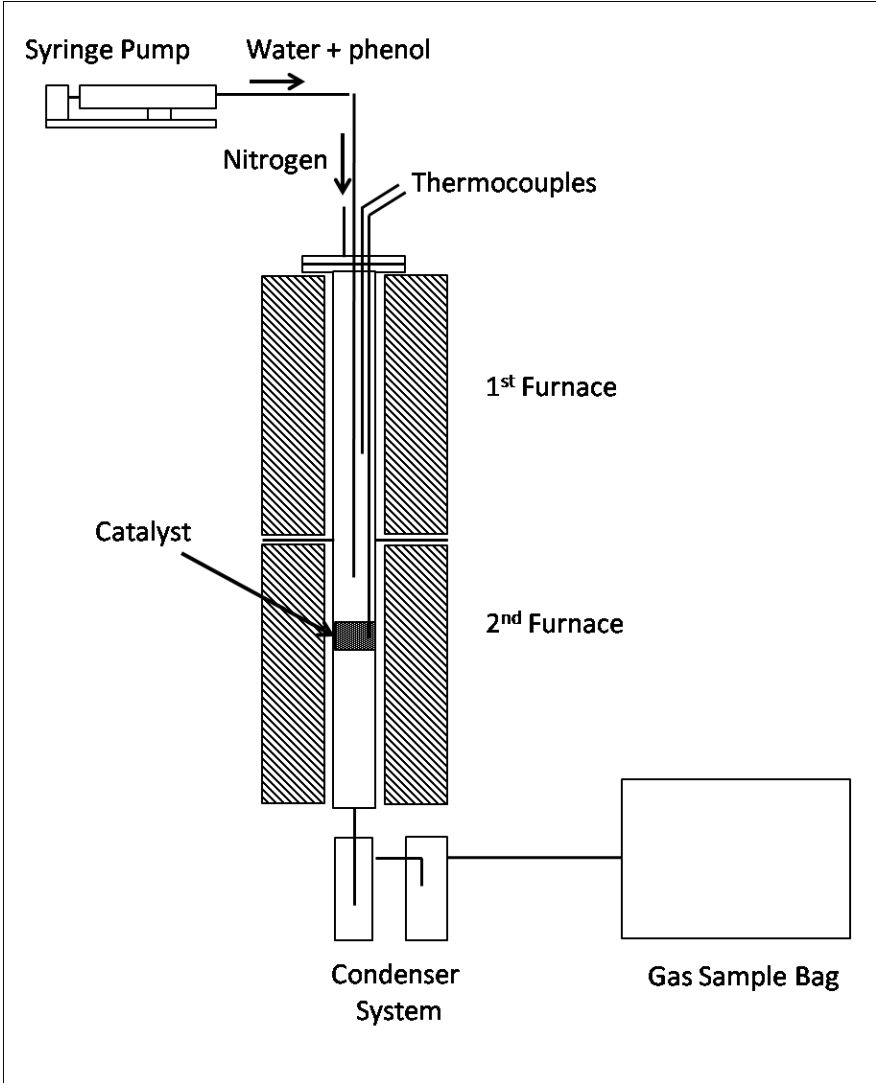
- 406 [17] Coll R, Salvado J, Farriol X, Montane D. Steam reforming model compounds of biomass
407 gasification tars: conversion at different operating conditions and tendency towards coke
408 formation. *Fuel Process Technol* 2001;74:19-31.
- 409 [18] Li C, Hirabayashi D, Suzuki K. Development of new nickel based catalyst for biomass tar
410 steam reforming producing H₂-rich syngas. *Fuel Process Technol* 2009;90:790-6.
- 411 [19] Zhang R, Wang H, Hou X. Catalytic reforming of toluene as tar model compound: Effect
412 of Ce and Ce-Mg promoter using Ni/olivine catalyst. *Chemosphere* 2014;97:40-6.
- 413 [20] Park HJ, Park SH, Sohn JM, Park J, Jeon JK, Kim SS, et al. Steam reforming of biomass
414 gasification tar using benzene as a model compound over various Ni supported metal
415 oxide catalysts. *Bioresour Technol* 2010;101:S101-3.
- 416 [21] Koike M, Ishikawa C, Li D, Wang L, Nakagawa Y, Tomishige K. Catalytic performance
417 of manganese-promoted nickel catalysts for the steam reforming of tar from biomass
418 pyrolysis to synthesis gas. *Fuel* 2013;103:122-9.
- 419 [22] Bona S, Guillen P, Alcalde JG, Garcia L, Bilbao R. Toluene steam reforming using
420 coprecipitated Ni/Al catalysts modified with lanthanum or cobalt. *Chem Eng Journal*
421 2008;137:587-97.
- 422 [23] Laosiripojana N, Sutthisripok W, Charojrochkul S, Assabumrungrat S. Development of
423 Ni-Fe bimetallic based catalysts for biomass tar cracking/reforming: Effects of catalyst
424 support and co-fed reactants on tar conversion characteristics. *Fuel Process Technol*
425 2014;127:26-32.
- 426 [24] Michel R, Lamacz A, Krzton A, Djéga-Mariadassou G, Burg P, Courson C, et al. Steam
427 reforming of α -methyl-naphthalene as a model tar compound over olivine and olivine
428 supported nickel. *Fuel* 2013 Jul;109:653-60.
- 429 [25] Shen Y, Chen M, Sun T, Jia J. Catalytic reforming of pyrolysis tar over metallic nickel
430 nanoparticles embedded in pyrochar. *Fuel* 2015;159:570-9.
- 431 [26] Ashok J, Kawi S. Steam reforming of toluene as a biomass tar model compound over
432 CeO₂ promoted Ni/CaO-Al₂O₃ catalytic systems. *Int J Hydrogen Energy*
433 2013;38:13938-49.
- 434 [27] Wang S, Zhang F, Cai Q, Li X, Zhu L, Wang Q, et al. Catalytic steam reforming of bio-
435 oil model compounds for hydrogen production over coal ash supported Ni catalyst. *Int J*
436 *Hydrogen Energy* 2014;39:2018-25.
- 437 [28] Wang S, Cai Q, Zhang F, Li X, Zhang L, Luo Z. Hydrogen production via catalytic
438 reforming of the bio-oil model compounds: Acetic acid, phenol and hydroxyacetone. *Int*
439 *J Hydrogen Energy* 2014;39:18675-87.
- 440 [29] Wu C, Williams PT. Hydrogen production by steam gasification of polypropylene with
441 various nickel catalysts. *Appl Catal, B* 2009;87:152-61.
- 442 [30] Efica CE, Wu C, Williams PT. Syngas production from pyrolysis-catalytic steam
443 reforming of waste biomass in a continuous screw kiln reactor. *J Anal Appl Pyrolysis*
444 2012;95:87-94.
- 445 [31] Polychronopoulou K, Bakandritsos A, Tzitzios V, Fierro JLG, Efstathiou AM.
446 Absorption-enhanced reforming of phenol by steam over supported Fe catalysts. *J Catal*
447 2006;241:132-48.

- 448 [32] Matas Guell B, Babich IV, Lefferts L, Seshan K. Steam reforming of phenol over Ni-
449 based catalysts - A comparative study. *Appl Catal, B* 2011;106:280-6.
- 450 [33] Wu C, Williams PT. Investigation of coke formation on Ni-Mg-Al catalyst for hydrogen
451 production from the catalytic steam pyrolysis-gasification of polypropylene. *Appl Catal,*
452 *B* 2010;96:198-207.
- 453 [34] Vicente J, Montero C, Ereña J, Azkoiti MJ, Bilbao J, Gayubo AG. Coke deactivation of
454 Ni and Co catalysts in ethanol steam reforming at mild temperatures in a fluidized bed
455 reactor. *Int J Hydrogen Energy* 2014;39:12586-96.
- 456 [35] Garbarino G, Sanchez Escribano V, Finocchio E, Busca G. Steam reforming of phenol-
457 ethanol mixture over 5% Ni/Al₂O₃. *Appl Catal, B* 2012;113-114:281-9.
- 458 [36] Remiro A, Valle B, Aguayo AT, Bilbao J, Gayubo AG. Operating conditions for
459 attenuating Ni/La₂O₃-Al₂O₃ catalyst deactivation in the steam reforming of bio-oil
460 aqueous fraction. *Fuel Process Technol* 2013;115:222-32.
- 461 [37] Clause O, Gazzano M, Trifiro F, Vaccari A, Zatorski L. Preparation and thermal
462 reactivity of nickel/chromium and nickel/aluminium hydrotalcite-type precursors. *Appl*
463 *Catal* 1991;73:217-36.
- 464 [38] Swierczynski D, Courson C, Kiennemann A. Study of steam reforming of toluene used as
465 model compound of tar produced by biomass gasification. *Chem Eng Process Process*
466 *Intensif* 2008;47:508-13.
- 467
- 468

469 **Figure captions**

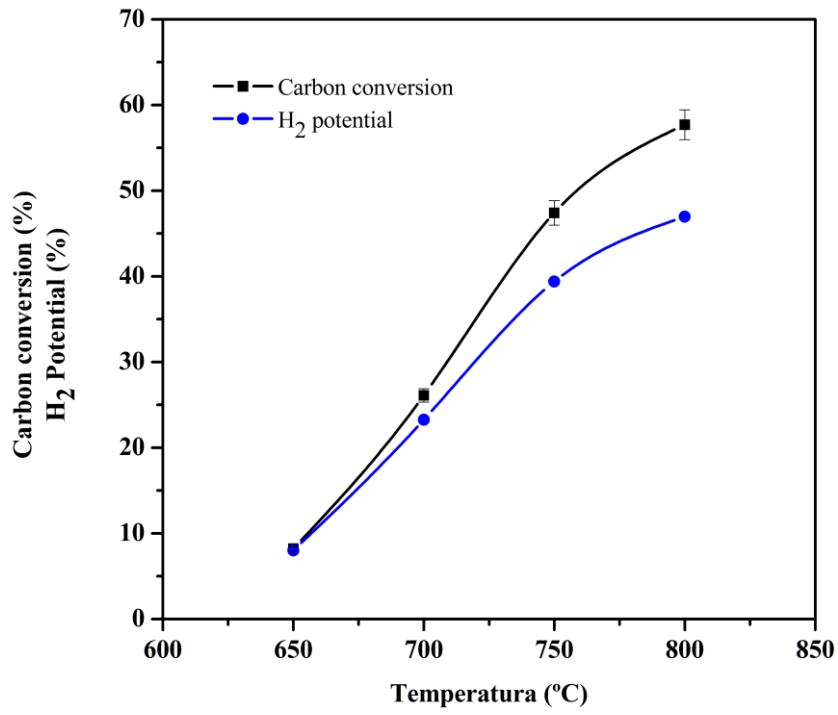
- 470 Figure 1. Experimental equipment used for steam reforming of phenol.
- 471 Figure 2. Effect of temperature on carbon conversion and H₂ potential (40 min; 1 g of
472 catalyst).
- 473 Figure 3. Effect of temperature on gas compounds yield (40 min; 1 g of catalyst).
- 474 Figure 4. DTG-TPO curves of the coke deposited over the catalyst used at different
475 temperatures (40 min; 1 g of catalyst).
- 476 Figure 5. SEM imagines of the fresh catalyst (a) and used catalyst at 650 (b), 750 (c)
477 and 800 °C (d) (40 min; 1 g of catalyst).
- 478 Figure 6. Effect of reaction time on carbon conversion and H₂ potential (750 °C; 1 g
479 of catalyst).
- 480 Figure 7. Effect of reaction time on gas compounds yield (750 °C; 1 g of catalyst).
- 481 Figure 8. DTG-TPO curves of the coke deposited over the catalyst used for different
482 reaction times (750 °C; 1 g of catalyst).
- 483 Figure 9. SEM imagines of the fresh catalyst (a) and used catalyst for 40 (b), 60 (c)
484 and 80 (d) min (750 °C; 1 g of catalyst).
- 485 Figure 10. Effect of catalyst amount on carbon conversion and H₂ potential (750 °C; 60
486 min).
- 487 Figure 11. Effect of catalyst amount on gas compounds yield (750 °C; 60 min).
- 488 Figure 12. DTG-TPO curves of the coke deposited over the catalyst used for different
489 catalyst amounts (750 °C; 60 min).

490



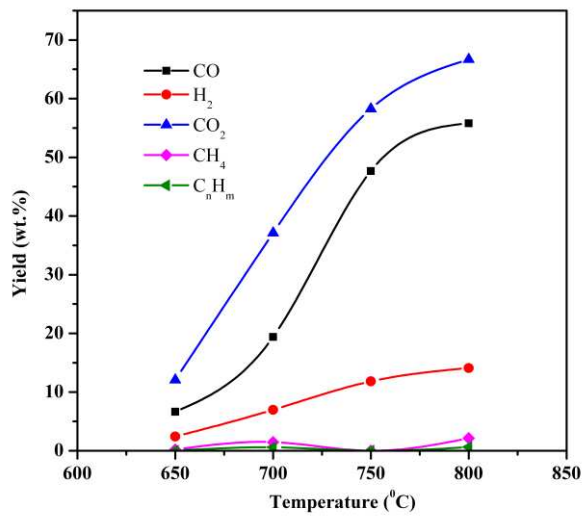
491

492



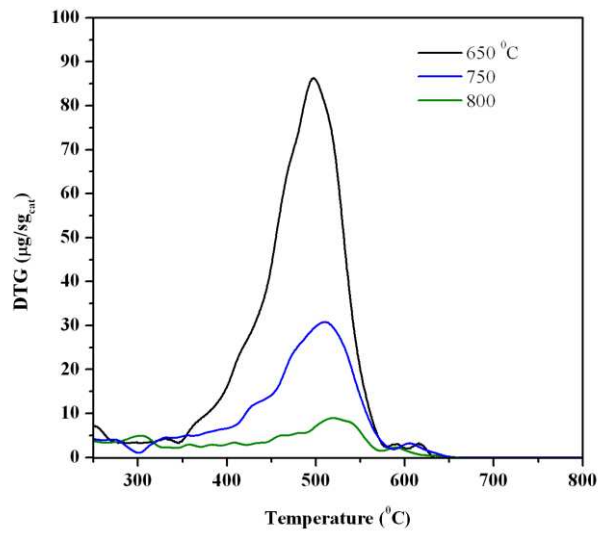
493

494



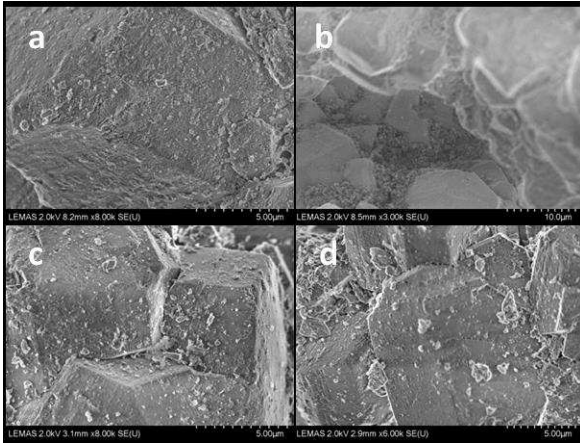
495

496



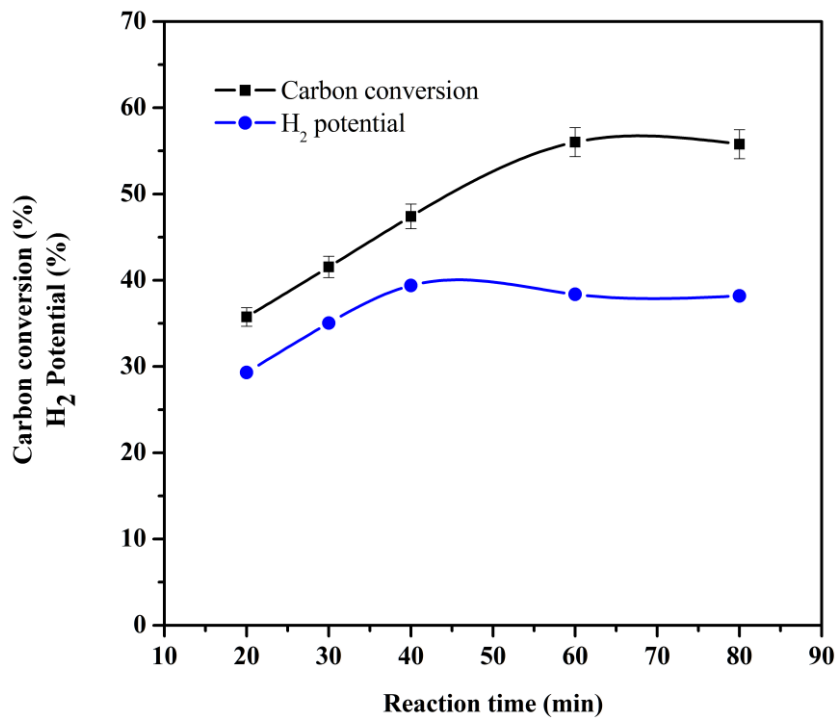
497

498



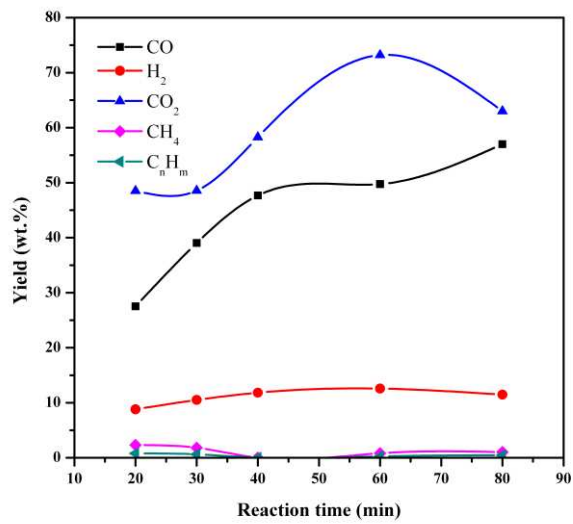
499

500



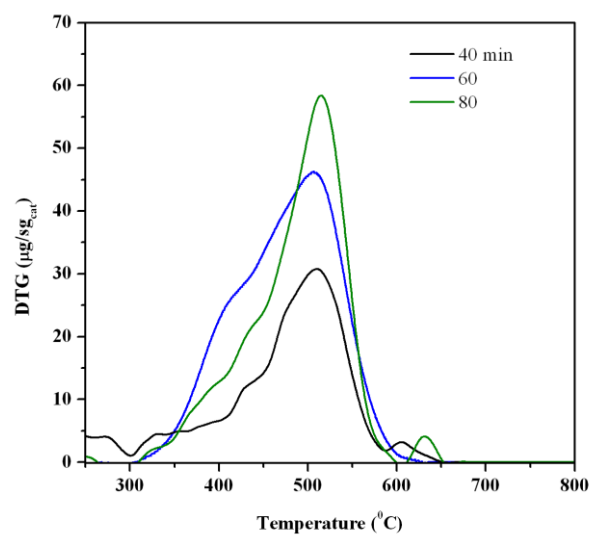
501

502



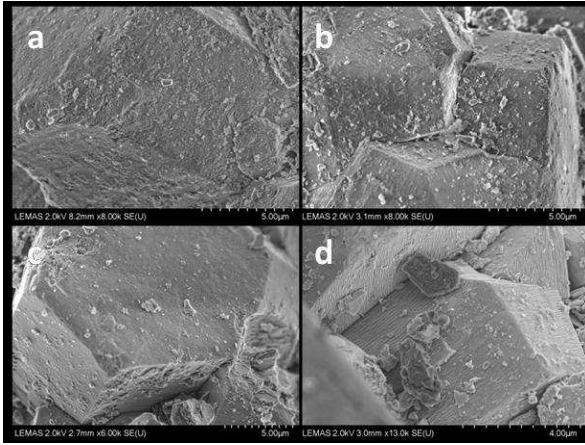
503

504



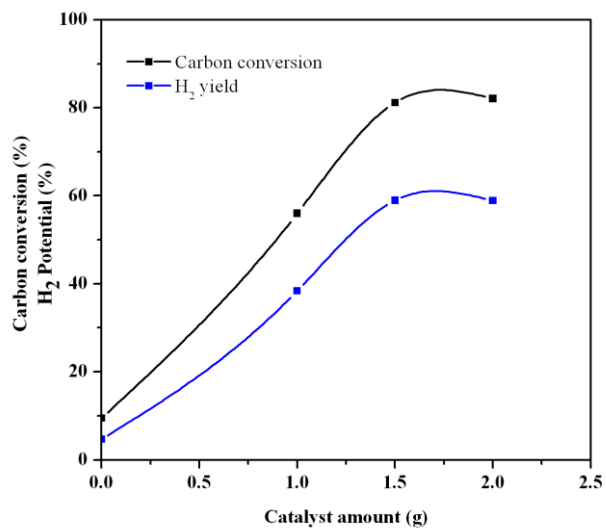
505

506



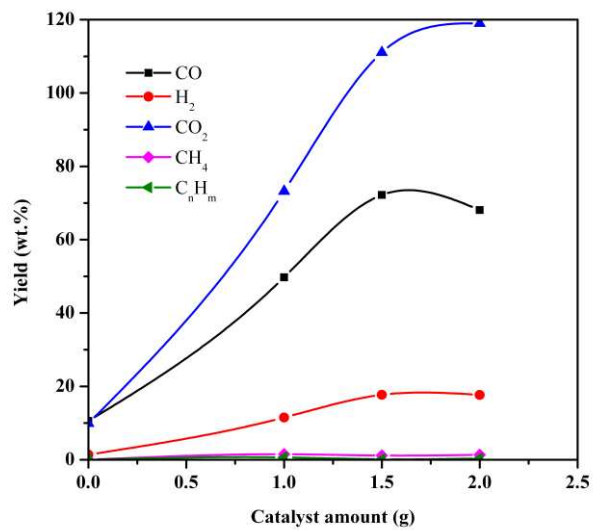
507

508



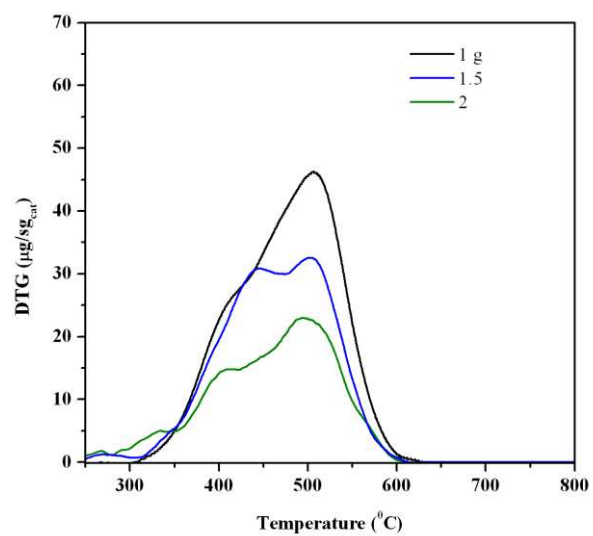
509

510



511

512



513

514

515